LIMNOLOGY
and
OCEANOGRAPHY: METHODS

Limnol. Oceanogr.: Methods 2, 2004, 356-364

High-frequency measurement of partial pressure and total concentration of carbon dioxide in seawater using microporous hydrophobic membrane contactors

Burke Hales[1], David Chipman[2], and Taro Takahashi[2]*
[1]College of Oceanic and Atmospheric Sciences, Oregon State University, Corvallis, OR 97331, USA
[2]Lamont-Doherty Earth Observatory of Columbia University, Palisades, NY 10964, USA

Abstract

To investigate CO_2 chemistry in ocean water with greater time-space resolutions, we developed measurement systems, which have state-of-the-art precision but an order of magnitude or better increase in the frequency of analysis, for carbon dioxide partial pressures (P_{CO2}) and total carbon dioxide concentrations (T_{CO2}) in seawater. The P_{CO2} system was based on equilibration of a CO_2-free carrier gas stream with aqueous carbon dioxide in a flowing seawater sample stream using a commercially available membrane contactor unit normally employed in industrial applications followed by nondispersive infrared (NDIR) absorbance detection of the CO_2 in the exit carrier gas. The T_{CO2} system was based on injection of a small-volume seawater sample loop (~1 mL) into an acid (0.1 N HCl) liquid carrier stream to convert all carbonate and bicarbonate ions to aqueous carbon dioxide; this acidified sample was then passed through a custom-made small-volume membrane contactor unit where the sample's P_{CO2} was determined by equilibration of a CO_2-free carrier gas followed by NDIR detection. Results from lab tests and a field experiment in the Ross Sea polynya, Antarctica, are presented. The P_{CO2} system was determined to have a response time of about 3 s and precision of better than 1 µatm. The T_{CO2} system had a maximum analysis rate of one sample per 36 s, and reproducibility was determined to be better than 0.2% for a period of hours.

As a result of various industrial activities, the CO_2 concentration in the earth's atmosphere increased by as much as 30% from the pre-industrial value of about 280 ppm (mole fraction in dry air) to about 375 ppm today. Presently, about 7 Petagrams (that is, 10^{15} g) of carbon are emitted into the earth's atmosphere annually. The rates of change in CO_2 and oxygen observed in the atmosphere in 1990s indicate that an amount of CO_2 equivalent to about one half of the annual CO_2 emissions is absorbed by the oceans and land ecosystems in nearly equal proportions (Keeling et al. 1996; Battle et al. 2000; Plattner et al. 2002; Keeling and Garcia 2002). The remaining half stays in the atmosphere. Thus, the global oceans play a major role in regulating the atmospheric CO_2 concentration, which affects the global heat balance and climate. Because the exchange of CO_2 between the atmosphere and the oceans occurs through the upper layers of the oceans and the CO_2 chemistry in seawater depends primarily on temperature and biological processes, it is important to understand regulatory mechanisms. Although the ocean as a whole is a net sink for atmospheric CO_2, the distribution of the ocean's sink and source areas varies in time and space as a result of complex interactions between photosynthetic fixation of CO_2, which consumes CO_2 in the photic zone, and vertical mixing, which supplies CO_2 and nutrients to the photic zone (Takahashi et al. 2002).

In seawater, CO_2 molecules react with water and are dissociated to three species: unhydrolized dissolved CO_2 ($CO_{2(aq)}$); bicarbonate ion ($HCO3^-$); and carbonate ion ($CO_3^=$). The total concentration of CO_2 dissolved in seawater (T_{CO2}) is the sum of the concentrations of all these species. In seawater, T_{CO2} ranges from 1800 µmol kg^{-1} in warm surface waters to 2400 µmol kg^{-1} in deep waters. About 1% of it is in the form of ($CO_{2(aq)}$), 2.5% is $CO_3^=$, and the remaining 96% is HCO_3^-; and the proportions change with temperature and pH. The partial pressure of CO_2 in seawater (P_{CO2}), which represents thermodynamic driving potential for CO_2 gas exchange across the sea-air interface, is simply proportional to the concentration of (CO_2)aq. When P_{CO2} and T_{CO2} in a parcel of water are measured, the CO_2 system in seawater is determined using known solubility of CO_2 (Weiss 1974) and the dissociation constants of carbonic acid

*Phone: (541) 737-8121. Fax: (541) 737-2064. E-mail: bhales@coas.oregonstate.edu

Acknowledgments

This work was supported by a grant from the National Science Foundation, OPP-9350684. This is LDEO Contribution Nr 6610.

in seawater (e.g., Millero et al. 2002). One of the unique features of CO_2 chemistry in seawater is that P_{CO2} is a sensitive function of T_{CO2}: $\partial \ln P_{CO2}/\partial \ln T_{CO2}$ called the Revelle factor, is 8 for warm waters and 15 for cold polar waters with high T_{CO2} concentrations. That is, a 1% change in T_{CO2} causes an 8% to 15% change in P_{CO2}. Accordingly, small changes in T_{CO2} may be detected by sensing the amplified changes in P_{CO2}. In this paper, we report rapid and high-precision measurement methods for P_{CO2} and T_{CO2} in seawater. These methods have been employed to investigate the sub-meso and mesoscale distributions of CO_2 chemistry in the upper layers of the oceans.

Materials and procedures

Objectives—To investigate the time-space distribution of CO_2 and nutrients in the upper layers of the oceans, we developed a hybrid towed undulating vehicle/continuous sampling system called the Lamont Pumping SeaSoar (LPS) (Hales and Takahashi 2002). The LPS is towed from a research vessel at speeds of 6 to 8 kts and undulates between the surface and ca 200 m depth at vertical ascent/descent rates of ca 20 m min^{-1}, all the while pumping a seawater flow of 8 linters min^{-1} back to the shipboard laboratory. In order to capture the rapid chemical changes present in the sample stream generated in this manner, the frequencies of chemical analyses needed to be increased dramatically from state of the art. We simultaneously developed a system for rapid nitrate, silicate, and phosphate analyses (Hales et al. 2004). Now our goal was to develop complementary P_{CO2} and T_{CO2} analyses that can attain vertical resolution equivalent to or better than that obtainable by hydrocast Niskin-bottle samples. This means that to maintain a vertical spacing of 10 m or less, we needed to develop systems that could perform at least two analyses per minute, all while maintaining the best possible accuracy and precision.

Principle of the systems—The systems we describe in subsequent sections are centrally dependent on equilibration of acidified and unperturbed seawater samples with carrier gases, via exchange of CO_2 across microporous hydrophobic membranes, which are then analyzed for their CO_2 content by NDIR absorbance. Gas-permeable membranes have been used in measurement of seawater P_{CO2} (e.g., Cai et al. 2000; DeGrandpre 1993; DeGrandpre et al. 1995, 1997, 1998, 2004; Hales et al. 1997; Ishiji et al. 2001; LeFevre et al. 1993; Wang et al. 2003; Zhao and Cai 1997). In these applications, (CO_2)aq in sample seawater was equilibrated across the membrane with a sensing aqueous solution, whose pH changed with changing (CO_2)aq or P_{CO2}. Because the equilibration took place via diffusion through aqueous media on both sides of solid gas-permeable membranes, the equilibration rate was on the order of min or longer. As a result, such systems have been deployed on moorings and on the seafloor in the deep ocean for sediment porewater measurement where the rapid response we seek is not as important. In contrast, in our application, the sensing medium was a gas and, hence, the transport-based response time would be about three orders of magnitude shorter because of the similarly higher diffusion coefficient in gases than in liquids.

Our search for raw membrane material led us to discover a newly formed branch of Hoechst (which has since become its own entity, Liqui-Cel; www.liquicel.com) specializing in gas-liquid contactor units for industrial applications. Many of their products are designed for much larger volume throughputs than we expected to use, however the smallest unit (LiquiCel 2.5 × 8) was about right for our P_{CO2} measurements made on the full 8 L min^{-1} LPS sample stream. This unit, which constituted the equilibrator for our P_{CO2} system, contains a bundle of approximately 10^4 X50® polypropylene tubes (220 micron inner diameter, 300 micron outer diameter, 50% porosity; *see* www.liquicel.com for more details) through which the carrier gas flows (the "lumenside"), while the seawater sample flows over the outside the tubes (the "shellside").

In contrast, our acidification approach to T_{CO2} measurement required a water flow rate of about 10 mL min^{-1}. Rather than optimizing our T_{CO2} measurement for higher flow rates, we took raw sample X50 tubing material (provided by T. Whisnant of Liqui-Cel) and constructed small-volume contactor units using bundles of about 10 of these tubes. In this system, a low-volume flow of acidified seawater sample was passed through the lumenside of the contactor unit and equilibrated with a carrier gas, which flowed through the shellside and was then analyzed for its CO_2 content by NDIR.

Hydrophobic membrane contactors similar to these have been used in measurement of SF_6 during deliberate tracer release experiments (e.g., Ho et al. 2002) and for lower temporal resolution surface P_{CO2} measurements (G. Friederich, Monterey Bay Aquarium Research Institution (MBARI), pers. comm. unref.), but their application to high-frequency measurement of P_{CO2} and T_{CO2} has not been discussed previously.

Analytical description—The two systems are schematically depicted in Fig. 1. The P_{CO2} system (Fig. 1A) is the simpler of the two, as the liquid flow path consists only of the main sample stream flowing through the shellside of Liqui-Cel 2.5 × 8 contactor unit. The carrier gas, dry N_2 in this case, flowed at a constant rate of about 150 mL min^{-1} through the lumenside of the contactor, opposite to the direction of seawater sample stream flow ("counter-flow"). After exiting the contactor, the now-equilibrated gas passed through a multi-position valve and then entered a 48-inch PermaPure (www.permapure.com) drying column where water vapor picked up in the contactor was removed, and finally flowed to a LI-COR 6251 NDIR absorbance unit (www.licor-env.com) for detection. Also plumbed to the multi-position valve was a set of five cylinders of known CO_2 content for regular, automated calibration of the LI-COR's nonlinear absorbance signal. The CO_2 concentration for each reference gas mixture is tied to the manometric measurements of C.D. Keeling (Scripps Institution of Oceanography). In addition to the output from the LI-COR unit, the temperature of the water flowing through the con-

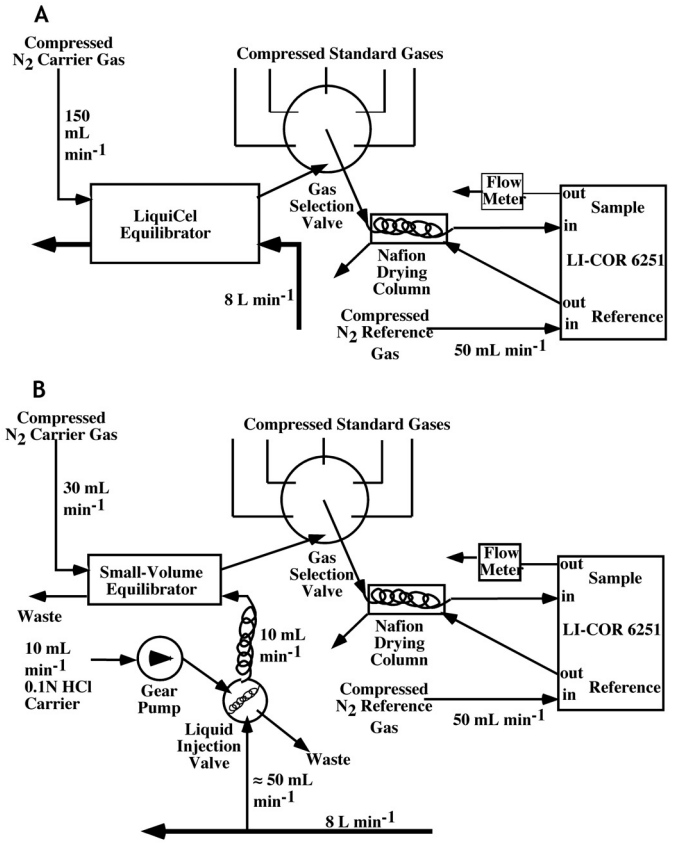

Fig. 1. Schematics of the (A) P_{CO2} and (B) T_{CO2} systems. The P_{CO2} system equilibrates a carrier gas with the entire, unmodified flow of the LPS (nominally 8 L min^{-1}) in a LiquiCel 2.5 × 8 membrane contactor unit. This equilibrated gas is then dried with dry N_2 contacted via a Nafion membrane and continuously analyzed with a LI-COR 6251 NDIR analyzer. The NDIR analyzer is calibrated with a suite of standard gases with known CO_2 content. The T_{CO2} analyzer, in contrast, draws a small split from the main LPS sample line, which flows through the sample loop of an injection valve. This sample is then injected into an acidified liquid carrier stream, which flows through a small, custom-made contactor unit consisting of a small bundle of the same hydrophobic microporous tubes as used in the commercial contactor. A carrier gas stream equilibrates with this acidified carrier/sample and is subsequently dried and then analyzed with a second calibrated LI-COR 6251 NDIR unit.

tactor, the shellside (carrier gas) pressure of the equilibrator (kept as low as possible), and the flow rate of the carrier gas are monitored and recorded. The sample's P_{CO2} at the sampling temperature is calculated from a second-order polynomial fit of the LI-COR output to the known standard gas concentrations for the three gases nearest the sample. Data were collected at the maximum frequency of the LI-COR unit, 0.5 Hz.

While the T_{CO2} system's gas flow path is virtually identical to that of the P_{CO2} carrier gas, the liquid flow is more complicated (Fig. 1B). Sample is driven by line pressure at a flow rate of about 50 mL/min from the main sample line, first through a multi-position valve and then to a two-position injection valve. When this second valve is in the "load" position, sample flows through an approximately 1-mL sample loop (made of a heavy-walled stainless steel tubing) on the valve and then to waste. When the injection valve was switched to the "inject" position, the sample loop was swept with an acidic (0.1 N HCl) carrier solution flowing at a rate of about 10 mL min^{-1}. The carrier/sample stream flowed through a 5-mL mixing coil to ensure complete acidification of the seawater sample loop, and then through the lumen-side of the custom small-volume contactor, and finally on to waste. Carrier gas (again, dry N_2) flows through the shellside of the contactor at 30 mL min^{-1} and, similar to the P_{CO2} system, through a drying column and multiposition standardization valve before entering a second LI-COR 6251 NDIR analyzer for analysis. As with the P_{CO2} system, liquid temperature, carrier gas pressure, and flow rate are monitored and recorded. While the NDIR system is calibrated in exactly the same manner as described above for P_{CO2}, the data analysis for T_{CO2} is different. Because the sample loop mixes axially with the carrier stream, the signal associated with each injected sample is an individual peak. Although we collected data at 0.5 Hz, and integration of the peaks was possible, we found that the best statistical representation of the data (as quantified by repeatability or linearity of calibration curves) came when the maximum peak height was used as the representation of the sample T_{CO2}. Liquid standardization was performed with 3 mixtures of known T_{CO2} concentration—prepared using $NaHCO_3$ solutions tied to pure Icelandic spar calcite solid standards—plumbed to the liquid multi-position valve and delivered by hydrostatic pressure because of the standards' elevation above the injection valve.

Results

Laboratory tests—We verified with laboratory tests that the two systems had acceptable analytical precision based on repeated analyses of the same test seawater sample: the P_{CO2} measurements were repeatable to 1 µatm or about 0.3% at atmospheric conditions. We verified absolute accuracy of the P_{CO2} system by comparison with standard large-volume equilibrator measurements of surface seawater in the field; this is discussed in detail in this section. We demonstrated by modeling the output signal response to a step-function change in inlet-water P_{CO2} that the P_{CO2} system had a response (e-folding) time of about 3 s, which we believe to be largely due to flushing of the LI-COR cell. The extent of equilibration of the P_{CO2} carrier gas stream with the liquid sample stream was verified by the equivalence, within our measurement precision, of P_{CO2} in the exit carrier gas whether the inlet gas P_{CO2} was significantly below (0 µatm N_2 carrier) or above (1000 µatm) the P_{CO2} of the test seawater sample stream. This is consistent with the expected millisecond-order gas transfer rates through the thin porous walls of the tubing. It is also consistent with the notion that the carrier gas stream does not significantly strip CO_2 from the seawater: at the gas and liquid flow rates used and extreme hypothetical combinations of low-CO_2 carrier and high-P_{CO2} seawater, less than 0.01% of the seawater T_{CO2} is removed by the carrier gas.

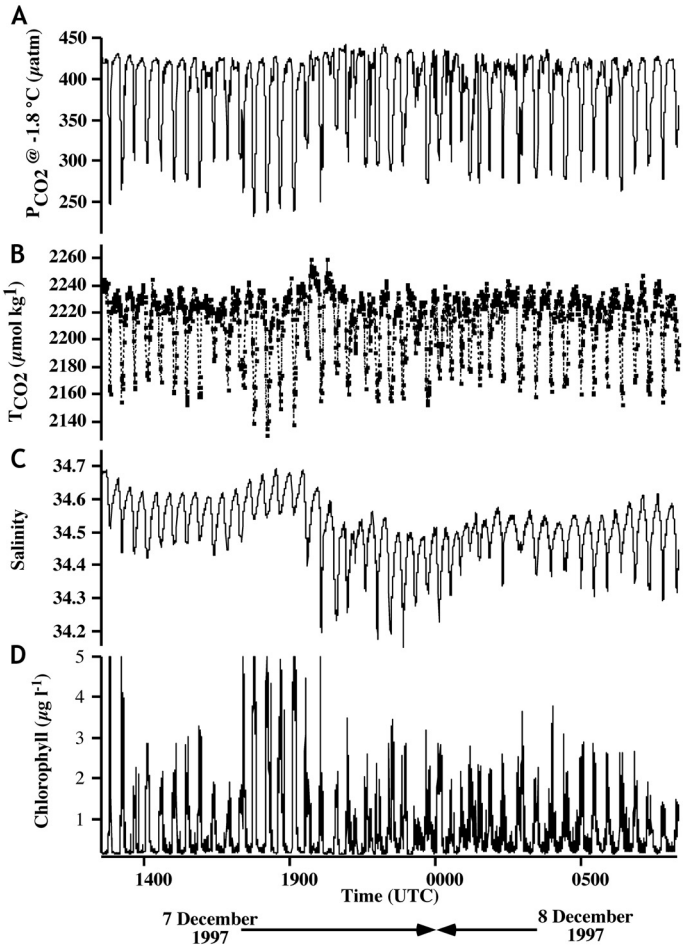

Fig. 2. Time-series measurements of (A) P_{CO2}, (B) T_{CO2}, (C) salinity, and (D) chlorophyll (from calibrated fluorometer) during a one-day deployment of the LPS in the Ross Sea polynya spanning 7–8 December 1997. P_{CO2} and T_{CO2} measurements, made with the analytical systems described here in the shipboard end of the LPS sample stream, were synchronized with the in situ measurements by comparing in situ and shipboard-measured salinity, as described by Hales and Takahashi (2002). Salinity and chlorophyll measurements were made with in situ sensors aboard the LPS.

Like the P_{CO2} system, laboratory tests showed that the T_{CO2} system's precision was adequate. Repeat measurements of the same seawater sample gave the same result to within 3 to 4 µmol kg^{-1} or ≤ 0.2%. Also like the P_{CO2} system, we attempted to verify the absolute accuracy with field tests. Unfortunately this proved problematic, and this is discussed in detail in subsequent sections. Axial smearing of the injected sample and the slower flushing rate of the LI-COR cell caused by the lower gas flow rate limited T_{CO2} sampling frequency to one analysis every 36 s. Samples injected more frequently were compromised by overlap of leading and trailing peak edges. Samples forced through the system faster, either by increased acid-carrier flow rates or decreased acid mixing coil volumes, did not completely and reproducibly acidify. Increased gas flow rates appeared to strip CO_2 from the acidified sample, thus invalidating the equilibration approach. Sample loops were flushed rapidly with respect to sampling period (flushing time of about 1 s) however, so the system's e-folding response time could well be shorter than the sampling period. At 36-s separation between injections there was no discernible "memory" of previous samples on current sample peak height. As a result, we cannot accurately quantify the system's response time. We know only that it must be several times shorter than the sample temporal separation. It is difficult to constrain the extent of equilibration of the acidified sample in the T_{CO2} system. It is acidified, and thus no longer possesses the buffering capacity of seawater. The gas:liquid flow ratios are substantially higher for the T_{CO2} system, and a simple mass-balance calculation shows that the carrier gas stream could potentially strip several percent of the acidified T_{CO2}. We tested for this by varying gas flow rates. At flows below 40 mL min^{-1}, we saw no sensitivity to further reductions in flow and felt that the 30 mL min^{-1} flow rate was safely within this limit.

Field data: Oceanographic results—We took these two systems to sea during the Joint Global Ocean Flux Survey (JGOFS) Antarctic Environment and Southern Ocean Process Study (AESOPS) Ross Sea Process IV cruise. The major objective of this expedition was to observe variability of biogeochemical properties in upper layers of water during the early stages of phytoplankton blooms in the highly productive Ross Sea shelf waters in the austral spring of 1997. The systems were operated during four 24-h surveys with the LPS. An example of the consistency between P_{CO2} and T_{CO2} measurements is shown in Fig. 2, along with the in situ measured physical and bio-optical parameters (salinity and fluorescence-based chlorophyll, respectively). The data were obtained during an approximately 20-h deployment between 170°E and 180°E longitude along 76.5°S latitude on 7 December 1997. The dominant temporal variability in all signals is due to the up-down cycling of the LPS from about 15 m to 190 m depths, with lower P_{CO2} and T_{CO2} coincident with lower salinity (and thus lower density) surface waters. These also have highest chlorophyll content. Other temporal structure is due to variable biological uptake of dissolved CO_2, as evidenced by the coherence between lowest values of surface P_{CO2} and T_{CO2} and highest values of surface chlorophyll.

Further illustrating the impact of physical and biological processes on these properties are the relationships between T_{CO2}, P_{CO2}, temperature, and salinity shown in Fig. 3. High chlorophyll waters (orange dots) have low P_{CO2} and T_{CO2} values, as expected from the photosynthetic use of CO_2. The low chlorophyll (purple dots) waters contain high P_{CO2} and T_{CO2} and represent the subsurface intrusion of Modified Circumpolar Deep Water, which is warmer than other water masses in the Ross Sea. As expected from the coherence between the patterns of T_{CO2} and P_{CO2} both with respect to time and temperature and from the early phytoplankton bloom in the Ross Sea (which is largely devoid of calcifying organisms), P_{CO2} and T_{CO2} are tightly correlated (Fig. 4). The slope of the near-linear relationship between the two variables corresponds to a

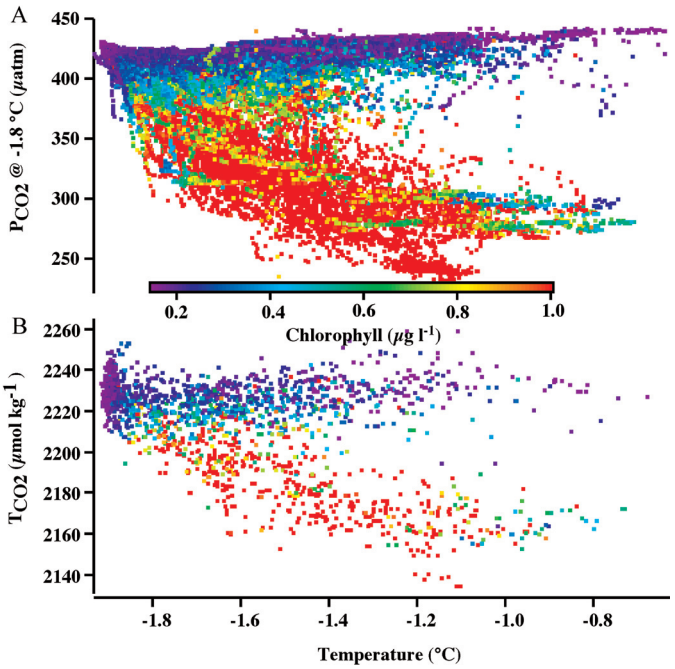

Fig. 3. Distributions of (A) P_{CO2} and (B) T_{CO2} as a function of temperature, with symbols colored as a function of co-located chlorophyll concentration. Both parameters exhibit conservative near-linear dependence on temperature when chlorophyll is low. Reflecting their consumption during photosynthesis, both parameters are strongly depleted relative to their simple dependence on temperature when coincidentally measured chlorophyll content is high.

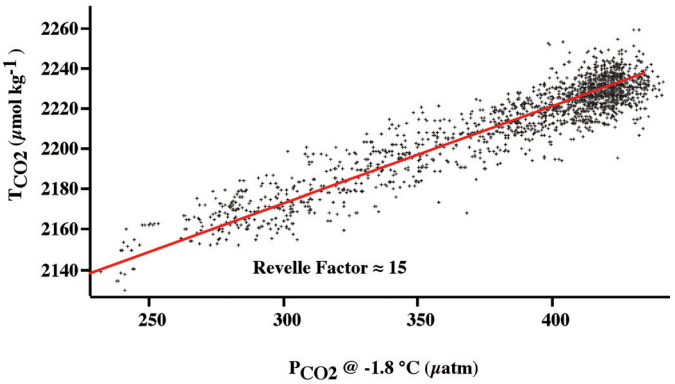

Fig. 4. Relationship between T_{CO2} and P_{CO2} for the entire transect sampled on 7 December 1997, spanning a depth-range of 10 to 180 m. The near-linear relationship between the two is consistent with a Revelle Factor of 15 (overlain solid line).

Revelle factor of about 15, consistent with 14.8 obtained on the basis of large-volume, coarse-resolution, discrete analyses of P_{CO2} and T_{CO2} in near surface waters south of 65°S (Morrison et al. 2001).

An example of the spatial variability present in distributions of such chemical parameters is the section of T_{CO2} concentrations given in Fig. 5. The well-resolved representation of the T_{CO2} distribution (Fig. 5a) shows striking finger-like vertical structures with horizontal scales so narrow that they are captured by only a few LPS tracks (spanning ca 20 km or less). It follows from the tight correlation of P_{CO2} and T_{CO2} shown above that corresponding P_{CO2} distributions are similarly spatially variable as Hales and Takahashi (in press) showed. Not only is the length scale of this variability short, its magnitude is large. They showed that the magnitude of the P_{CO2} variability at these short length-scales is tens of µatm. This is supported by the time-series data shown in Fig. 2, where it is clear that surface P_{CO2} has a range of 100 µatm, which is sometimes experienced in the space of only ca 10 km. The similarly large amplitude of T_{CO2} variability expected from tight coupling between P_{CO2} and T_{CO2} is borne out by the time series distributions of Fig. 2 and the highly-resolved section of Fig. 5A. T_{CO2} at a given depth can vary by up to 50 µmol kg^{-1}, and, again, this entire range can be experienced in lateral distances of only ca 10 km.

In dramatic contrast to the picture provided by the high-resolution LPS-based sampling and high frequency analyses described here is the distribution of T_{CO2} that would be assumed based on T_{CO2} measurements of samples collected from typical 50 km-resolution hydrostation Niskin-bottle sampling (Fig. 5B). This representation misses most of the variability in the distribution and imposes lateral connections

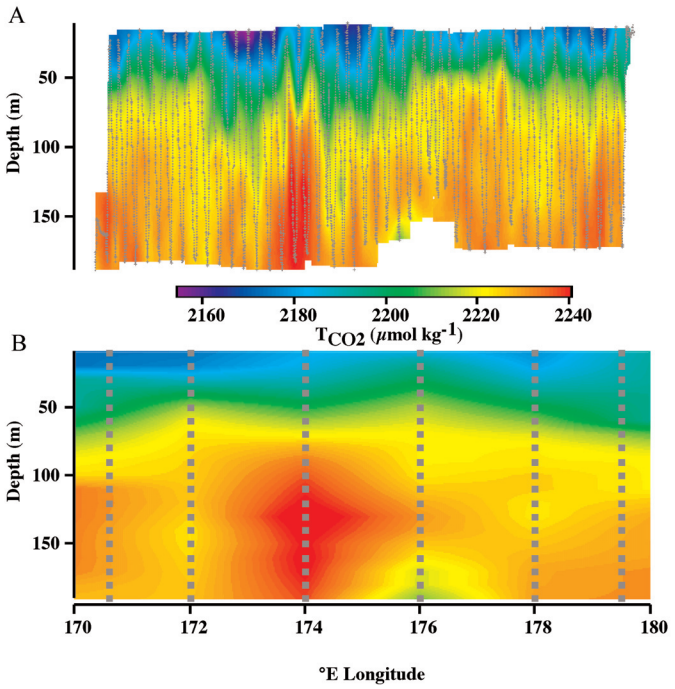

Fig. 5. Longitude- and depth-dependent sections of (A) T_{CO2} as observed with the LPS and the analytical system described here, and (B) T_{CO2} as it would appear based on a coarse resampling of (A). In (A), the small symbols connected with the light solid line demonstrate the measurement density of the LPS-based T_{CO2} data. In (B), the larger squares show the locations of subsamples extracted from the highly-resolved grid in (A). These extracted samples were selected to approximate hydrostation style sampling.

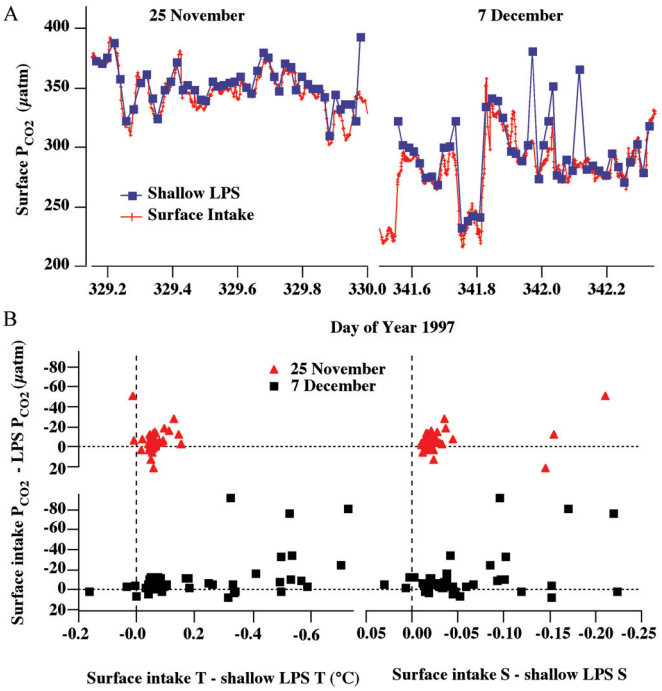

Fig. 6. (A) Field-study ground-truthing of P_{CO2} based on comparison of LPS-based surface P_{CO2} (large blue symbols/lines) with more traditional large-volume showerhead-style equilibration of surface water drawn by the ship's uncontaminated seawater (USW) intake. Comparisons are made for a transect completed early in the bloom initiation period shortly after a strong wind-forcing event (LPS mimimum depth = 20 ± 2 m) and for a transect 2 weeks later following consistently mild winds and much greater expression of phytoplankton growth (LPS mimimum depth = 15 ± 2 m). P_{CO2} measured by the two methods is, in general, in good agreement; the few instances of large deviation come when the deviation between ship's USW-based and LPS-based temperature and salinity is greatest (B). The frequency of these water-mass property deviations is greatest for the latter transect, despite the shallower minimum LPS depths achieved then, leading us to believe that the establishment of very shallow surface mixed layers has become more important over time.

between widely separated samples that simply do not exist in the well-resolved distributions.

Field data: Verification of system accuracies—P_{CO2}. Performing these measurements within the context of a larger program where traditional sampling and analyses were being performed aboard the same ship gave us the ability to rigorously verify the accuracy of these new approaches with direct comparisons to analyses by established procedures. We compared P_{CO2} measured on near-surface LPS samples with that measured at the same time and place by a large-volume showerhead equilibrator (Broecker and Takahashi 1966; Takahashi et al. 1998) inline with the ship's continuous underway uncontaminated surface-water (USW) sample intake (Fig. 6a). With a few exceptions, the agreement between these two independent measures of a highly variable P_{CO2} distribution is extremely good. The variability implied by the LPS-based membrane equilibrator measurements is supported by the USW-based large-volume equilibrator data, and the two sets of measurements are generally in phase.

There are some exceptions to this positive result, all of which are characterized by the LPS-based measurement substantially exceeding the USW-based result. This is sometimes by an amount in excess of 80 µatm and occurs more frequently in the later transect. We believe this is a result of establishment of very shallow mixed layers, which the LPS could not effectively sample with its nominal 15 to 20 m minimum depth. This is supported by Fig. 6B, which shows that the largest deviations between the two P_{CO2} measurements always come when the difference between temperature and/or salinity measured in the ship's surface intake line and those measured by the LPS was largest. Formation of such shallow mixed layers could be possible in this setting: these surveys took place during austral spring when the Ross Sea polynya was widening due to ice-melt caused by increasing insulation, so input of low-salinity, buoyant water at the surface could cause shallow stratification. In addition, the first of these two transects immediately followed a large wind event, while the second followed the ensuing 2 weeks of very calm weather. Despite the fact that the LPS reached shallower minimum depths during the second transect (15 ± 2 m) than on the first (20 ± 2 m), the frequency of disagreement between USW- and LPS-based T, S, and P_{CO2} is greater for the second transect. This supports the notion that formation of very shallow surface mixed layers had increased over this time period. Sampling such shallow mixed layers with vehicles that are, in all likelihood within the wake of the towing ship while near the surface, is of course impossible with ship's hull drafts approaching 10 m. These scenarios demonstrate the importance of incorporating data from surface USW intake lines when the very near-surface water properties are of interest.

The magnitude of these disagreements is greatly reduced when accounting for the offset between physical properties of LPS and USW samples. When limiting the comparison to USW and LPS sampled waters whose temperatures are within 0.3% and salinities are within 0.1 of each other, P_{CO2} measured by the methods presented here is 5.3 ± 7 (n = 44) and 4.4 ± 5 (n = 25) µatm higher than that measured by the large-volume equilibrator for the 25 November and 7 December 1997 transects, respectively. Further limiting the comparison to samples with better temperature agreement reduces this difference to 4.6 ± 6 (n = 42) and 3.5 ± 5 (n = 18) µatm for samples within 0.1°C of each other on the two transects, respectively, and to 2.4 ± 7 (n = 10) and 2.4 ± 6 (n = 8) µatm for samples within 0.05°C. We are unsure of the implication of the nonzero differences attained, even when the T and S characteristics of the water masses were significantly limited. This is clearly a setting with extreme spatial variability, and expectation of perfect agreement may be unjustified—the deviations between the two systems are certainly not statistically significantly different from zero, even in fairly permissive T and S agreement restrictions.

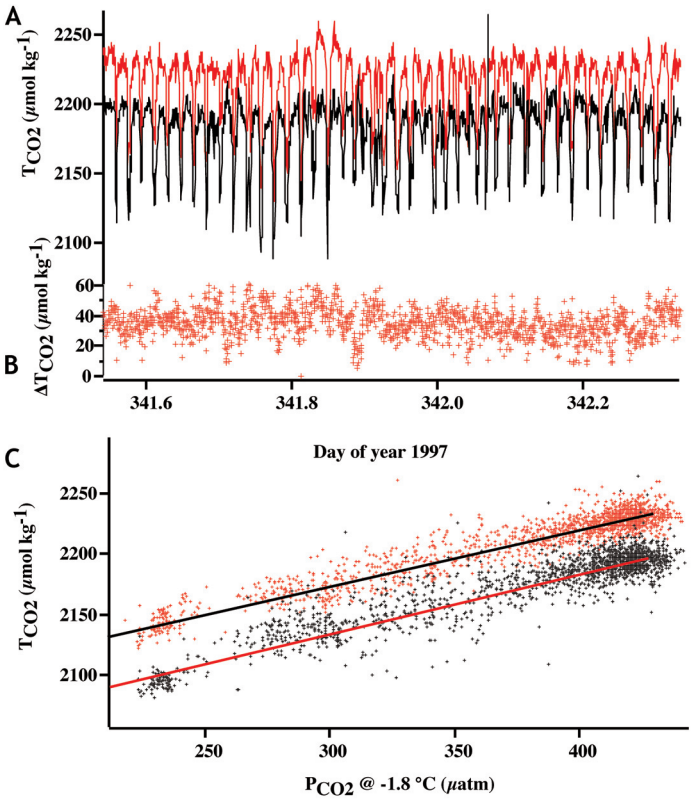

Fig. 7. Time-series of (A) T_{CO2} measured by two supposedly identical systems (red trace is the same as plotted in Fig. 2B) and (B) the difference between the two systems' measurements. (C) Comparison of the two T_{CO2} estimates as a function of P_{CO2}. Both show similar Revelle factor relative dependences on P_{CO2} (overlain light solid lines correspond to a Revelle factor of ~15, as in Fig. 2) but the RMS deviation of the second system about its mean trend is larger than for the first.

Alternatively, disagreements of this magnitude may be accounted for by calibration errors of only about 0.2°C between the USW and LPS temperature sensors. We cannot, with this data, further resolve the agreement, or lack thereof, between the two systems and simply state that the rapid membrane-contactor–based analysis of P_{CO2} in LPS samples agrees with traditional approaches to within a couple of µatm; even this difference may not be significant.

T_{CO2}. Discussion of T_{CO2} data to this point has been based on measurements made with one system as described earlier, which yielded T_{CO2} values consistent with the values obtained using a coulometric system (Chipman et al. 1993). The coulometer system was calibrated using a known number of moles of 99.98% purity CO_2 gas, and yielded TCO_2 values consistent with reference solutions provided by A.G. Dickson of the Scripps Institution of Oceanography. Because the T_{CO2} values in these reference solutions were determined using the manometric method of C.D. Keeling (Scripps Institution of Oceanography), our P_{CO2} and T_{CO2} values are both tied to his manometric measurements.

Unfortunately we built a second system, which was used along with the first to double the analysis frequency. Here, we encountered difficulties. We calibrated this supposedly identical system in exactly the same manner as the first, using the same standard solutions and gases, and operated them in parallel during the transect discussed earlier. Comparison of T_{CO2} measured with the two systems is shown in Fig. 7. The offset between the two is large. T_{CO2} measured with the second system was on average 35 ± 8 µmol kg^{-1} lower than that measured with the first. This difference, about 1.6%, far exceeds precisions and is inconsistent with the accuracy required to make meaningful comparisons of our data with those of other researchers.

It is tempting to simply ignore the results of the second system—they are noisier with respect to P_{CO2} (RMS deviations from Revelle lines shown in Fig. 7C are 9 and 17 µmol kg^{-1} for the first and second systems, respectively), and the second system appears to be in greater disagreement with hydrographic data than the first. The fact remains, however, that the two systems were intended to be identical and were calibrated in exactly the same way. Their internal disagreement suggests a fundamental difference in the ways we treat standards and samples and casts doubt on any claims we might make about absolute accuracy. We must therefore be satisfied with the internal consistency between the relative variability recorded by the T_{CO2} system and other independent measures of biogeochemical variability in the Ross Sea. Attaining acceptable absolute accuracy is left for further development.

Comments and recommendations

The obvious shortcoming of the analytical results presented here lies in the internal inconsistency of the T_{CO2} data collected by two supposedly identical systems. We can postulate reasons that a single system might be in error. For example, CO_2 in the seawater sample loop, diluted with and acidified by the carrier solution, is not well buffered (as in seawater), and the higher gas:liquid flow ratios in the T_{CO2} contactor unit may act to strip CO_2 from the liquid stream rather than simply equilibrating with it. This introduces the potential for elevated sensitivity to flow rates and mixing ratios. Alternatively, there may be uncertainties that are unaccounted for in the temperature measurements of the carrier/sample stream. Because the sample is completely acidified, there is no Revelle-factor damping of the sensitivity to CO_2 solubility. The 1.6% offset could be due to a temperature inaccuracy of less than 0.4°C. Whereas these might explain deviation from theoretical performance, none can explain how two supposedly identical analyses calibrated with the same standards can give systematically different answers. This problem must be resolved before the methods presented here can aspire to state-of-the-art T_{CO2} measurement accuracy.

Despite these problems, we do believe that the relative variability determined by both systems is correct. Therefore, this approach could be used in situations where the relative

variability is large compared to the order 1% accuracy uncertainty, such as estuaries, river plumes, or stratified lakes. In addition, the approach of injecting small volumes has application to measurement of samples such as those collected in porewaters or benthic flux-chamber incubation experiments where sample sizes are small, variability is large, and relative changes are important.

Conclusions

We have developed systems for rapid, precise, and accurate measurement of P_{CO2}, and rapid and precise measurement of T_{CO2}. We validated these systems, interfaced with the sample stream generated by the Lamont Pumping SeaSoar, during fieldwork in the Ross Sea polynya during austral summer of 1997. High-resolution measurements of these systems show very short horizontal-scale variability that could not be observed with traditional hydrostation sample spacing. Field accuracy for P_{CO2} was verified by comparison of surface samples measured in the manner described above with traditional large-volume showerhead-style equilibration of surface waters sampled by the ship's surface water intake. Accuracy of T_{CO2} was unsatisfactory, given the 1.6% disagreement between two supposedly identical T_{CO2} rapid-analysis systems.

References

Battle, M., M. L. Bender, P. P. Tans, J. W. C. White, J. T. Ellis, T. Conway, and R. J. Francey. 2000. Global carbon sinks and their variability inferred from atmospheric O_2 and $\delta^{13}C$. Science 287:2467-2470.

Broecker, W. S., and T. Takahashi. 1966. Calcium carbonate precipitation on the Bahama Banks. J. Geophys. Res. 71: 1575-1602.

Cai, W. -J., P. Zhao, and Y. Wang. 2000. pH and pCO_2 microelectrodes measurement and diffusive behavior of carbon dioxide species in coastal marine sediments. Mar. Chem. 70:133-148.

Chipman, D. W., J. Marra, and T. Takahashi. 1993. Primary production at 47°N and 20°W in the North Atlantic Ocean: A comparison between the ^{14}C incubation method and the mixed layer carbon budget. Deep-Sea. Res. 40 (1/2):151-169.

DeGrandpre, M. D. 1993. Measurement of seawater P_{CO2} using a renewable-reagent fiber-optic sensor with colorimetric detection. Anal. Chem. 65:331-337.

———, T. R. Hammar, S. P. Smith, and F. L. Sayles. 1995. In situ measurements of seawater pCO_2. Limnol. Oceanogr. 40: 969-975.

———, T. R. Hammar, D. W. R. Wallace, and C. D. Wirick. 1997. Simultaneous mooring-based measurements of seawater CO_2 and O_2 off Cape Hatteras, North Carolina. Limnol. Oceanogr. 42:21-28.

———, T. R. Hammar, and C. D. Wirick. 1998. Short term pCO_2 and O_2 dynamics in California coastal waters. Deep-Sea Res. II 45:1557-1575.

———, R. Wanninkhof, W. R. McGillis, and P. Strutton. 2004. A Lagrangian study of pCO_2 dynamics in the eastern equatorial Pacific Ocean, submitted to *Journal Geophysical Research* 109:C08S07, doi:10.1029/2003JC002089.

Hales, B., L. Burgess, and S. R. Emerson. 1997. An absorbance-based fiber-optic sensor for CO_2(aq) measurement in porewaters of sea floor sediments. Marine Chem. 59:51-62.

——— and T. Takahashi. 2002. The pumping SeaSoar: A high-resolution seawater sampling platform. J. Ocean. Atmos. Technol. 19:1096-1104.

———, A. van Geen, and T. Takahashi. 2004. High-frequency measurement of seawater chemistry: Flow-injection analysis of macronutrients. Limnol. Oceanogr.:Methods 2:91-101.

——— and T. Takahashi. 2004. High-resolution biogeochemical investigation of the Ross Sea, Antarctica, during the AESOPS (U.S. JGOFS) program. Global Biogeochem. Cycles 18:GB3006, doi:10.1029/2003GB002165.

Ho, D. T., P. Schlosser, and T. Caplow. 2002. Determination of longitudinal dispersion coefficient and net advection in the tidal Hudson River with a large-scale, high resolution SF6 tracer release experiment. Environ. Sci. Technol. 36: 3234-3241.

Ishiji, T., D. W. Chipman, T. Takahashi, and K. Takahashi. 2001. Amperometric sensor for monitoring of dissolved carbon dioxide in seawater. Sensors Actuat. B76:265-269.

Keeling, R., S. C. Piper, and M. Heinmann. 1996. Global and hemispheric CO_2 sinks deduced from changes in atmospheric O_2 concentration. Nature 381:218-221.

Keeling, R. F., and H. Garcia. 2002. The change in oceanic O_2 inventory associated with recent global warming. Proc. U. S. Nat. Acad. Sci. 99:7848-7853.

LeFevre, N., J. P. Ciabrini, G. Michard, B. Brient, M. DuChauffat, and L. Merlivat. 1993. A new optical sensor for P_{CO2} measurements in seawater. Mar. Chem. 42:189-198.

Millero, F. J., J. -Z. Zhang, D. Pierrot, K. Lee, R. Wanninkhof, R. Feely, C. L. Sabine, R. M. Key, and T. Takahashi. 2002. Dissociation constants for carbonic acid determined from field measurements. Deep-Sea Res. II 49:1705-1723.

Morrison, J. M., S. Gaurin, L. A. Codispoti, F. J. Millero, T. Takahashi, W. D. Gardner, and M. J. Richardson. 2001. Seasonal evolution of hydrographic properties in the Antarctic circumpolar current at 170°W during 1997-1998. Deep-Sea Res. II 48:3943-3972.

Plattner, G. -K., F. Joos, and T. F. Stocker. 2002. Revision of the global carbon budget due to changing air-sea oxygen fluxes. Glob. Biogeochem. Cycles 16:1096. DOI: 10.1029/2001GB001746.

Takahashi, T., D. W. Chipman, S. Rubin, J. Goddard, and S. C. Sutherland. 1998. Measurements of the total CO_2 concentration and partial pressure of CO_2 in seawater during WOCE Expeditions P-16, P-17 and P-19 in the South Pacific Ocean, October 1992–April 1993. Final Technical Report of Grant No. DE-FGO2-93ER61539 to U. S. Department of

Energy, Lamont-Doherty Earth Observatory, Palisades, NY 10964, pp. 124.

———, S. C. Sutherland, C. Sweeney, A. Poisson, N. Metzl, B. Tillbrook, N. Bates, R. Wanninkhof, R. A. Feely, C. Sabine, J. Olafsson, and Y. Nojiri. 2002. Global sea-air CO_2 flux based on climatological surface ocean pCO_2, and seasonal biological and temperature effects. Deep-Sea Res. II. 49:1601-1622.

Wang, Z., W.-J. Cai,. and Y. Wang. 2003. Spectrophotometric pCO_2 measurements based on a long pathlength liquid-core waveguide in the South Atlantic Bight. Mar. Chem. 84:73-84.

Weiss, R. F. 1974. Carbon dioxide in water and seawater: The solubility of a non-ideal gas. Mar. Chem. 2:203-215

Zhao, P., and W. -J. Cai. 1997. An improved potentiometric pCO_2 microelectrode. Anal. Chem. 69:5052-58.

Submitted 23 July 2004
Revised 20 August 2004
Accepted 26 August 2004